

## ***Supporting Information***

### **Utilizing decavanadate as an artificial solid electrolyte interface to effectively suppress dendrite formation on lithium metal anode**

*Jian Song,<sup>ab</sup> Yuanyuan Jiang,<sup>a</sup> Yizhong Lu,<sup>\*a</sup> Changhao Zhao,<sup>a</sup> Yundong Cao,<sup>a</sup> Linlin Fan,<sup>\*a</sup> Hong Liu<sup>a</sup> and Guanggang Gao<sup>\*a</sup>*

<sup>a</sup>School of Materials Science and Engineering, University of Jinan, Jinan 250022, China

<sup>b</sup>Linyi Vocational University of Science and Technology, Linyi 276025, China

\*Corresponding authors

E-mail: mse\_luyz@ujn.edu.cn (Yizhong Lu); mse\_fanll@ujn.edu.cn (Linlin Fan);  
mse\_gaogg@ujn.edu.cn (Guanggang Gao)

## 1. Experimental section

**Synthesis of V<sub>10</sub>:** Na<sub>6</sub>V<sub>10</sub>O<sub>28</sub>·18H<sub>2</sub>O (V<sub>10</sub>) was prepared based on the method previously reported with further optimized.<sup>[41]</sup> 3 g of NaVO<sub>3</sub> was dissolved in 100 mL distilled water, then 4 M HCl solution was added dropwise to reduce the pH to 4.8. After filtering the above solution, continue to add HCl solution to maintain the pH value at 4.5. Subsequently, 200 mL of 95% ethanol was added to the above solution, and let it stand for 3 days to obtain the V<sub>10</sub> crystals.

**Preparation of V<sub>10</sub> modified lithium foils:** V<sub>10</sub> was added to the DOL/DME solution (volume ratio of 1:1) under ultrasonication for 1 h to obtain the uniform V<sub>10</sub> suspension. Subsequently, lithium foils were immersed in the above solution and stirred for 24 h to obtain V<sub>10</sub> modified lithium foils.

**Cell assembly and electrochemical measurement:** The Li//Li symmetric cells were assembled using pristine lithium foil or V<sub>10</sub> modified lithium foil as electrode. For Li//Cu half cells, Cu foil was used as the working electrode and pristine Li foil or V<sub>10</sub> modified lithium foil was used as the counter/reference electrode. The electrolyte contained 1.0 M LiTFSI dissolved in the binary solvent of 1,3-dioxolane (DOL) and 1,2-dimethoxyethane (DME) (1:1 in volume) with 1.0 wt% LiNO<sub>3</sub>, and 30 μL electrolyte was added in each cell. For Li-S cells, the cathode was prepared by casting a paste that consisted of KB/S and LA133 (5.0 wt%) (mass ratio of 94:6) onto an aluminum foil. The coated electrodes were dried in a vacuum oven at 60 °C overnight and punched into a Ø10 mm circular membrane. The areal loading of active sulfur was 2.1 mg cm<sup>-2</sup>. Pristine lithium foil or V<sub>10</sub> modified lithium foil was used as the anode, and the cell contained an electrolyte to sulfur ratio of 10 μL mg<sup>-1</sup>. DH7006 electrochemical workstation (Jiangsu Donghua Analytical Instrument Co., Ltd, Donghua Analytical) was used to test CV and EIS in the frequency range of 100 kHz-0.01Hz with a voltage amplitude of 5 mV. The cycle performance and rate performance tests of the Li//Li and Li-S cells were carried out on the Neware battery test system (CT-4008-5V50mA-164, Shenzhen Neware Electronics

Co., Ltd., China). Li//Cu half cells were assembled to test the nucleation overpotential and Coulombic efficiency. All the above cells (CR2032) were assembled in a glove box filled up with argon ( $O_2 < 0.1$  ppm,  $H_2O < 0.1$  ppm).

**Materials characterization:** The microstructures and elemental mappings of  $V_{10}$  modified lithium foils were obtained via scanning electron microscope (SEM, Zeiss Ultra 55 field-emission gun). X-ray diffraction (XRD) was detected by Bruker D8 Advance. X-ray photoelectron spectroscopy (XPS) was recorded on an ESCA Lab MKII X-ray photoelectron spectrometer with non-monochromatized Mg  $K\alpha$  X-rays as the excitation source. Fourier transform infrared spectroscopy (FTIR) was obtained using a NEXUS-870 spectrophotometer with KBr pellets. Contact angles were detected by a POWEREACH JC2000D2G instrument. In-situ optical microscopy studies of Li//Li symmetrical cells were performed in transparent glass cell (Beijing Scistar Technology Co., Ltd.) viewed by an optical microscopy. Sulfur content in KB/S composite was confirmed under  $N_2$  atmosphere via the Thermogravimetric analysis (TGA) at a heating rate of  $10\text{ }^\circ\text{C min}^{-1}$  on TA Instrument Q 600 Analyzer. In-situ Raman test was performed in a Raman lithium ion battery (Beijing Scistar Technology Co., Ltd.) using a Raman spectrometer (Labramis, Horiba Jobbin Yvon, Paris, France) with wavelength of 532 nm.

**Preparation of sulfur cathode:** The melt-diffusion method was used to infiltrate the appropriate amount sulfur into KB. The KB and S were uniformly mixed with a weight ratio of 3:7, and the resulted products were heated at  $155\text{ }^\circ\text{C}$  for 12 h under Ar atmosphere to obtain the KB/S composite.

**Part of the formula:**

$R_0$  and  $R_s$  refer to the interfacial resistance before and after AC impedance.  $I_0$  and  $I_s$  represent the current value in initial and steady state under a polarization potential of 10 mV.  $t_{Li^+}$  is the lithium transfer number, and the value is calculated as follows.

$$t_{Li}^+ = \frac{I_s(\Delta V - I_0 R_0)}{I_0(\Delta V - I_s R_s)} \quad (S1)$$

The  $t_{Li}^+$  is largely enhanced, which prolongs the ‘‘Sand's time’’ of lithium dendrites nucleation according to Sand's formula as described below:

$$t_{sand} = \pi D_{app} \frac{(Z_c C_0 F)^2}{4(J t_a)^2} \quad (S2)$$

where  $D_{app}$  represents the apparent diffusion coefficient,  $Z_c$  is the charge number of the cation ( $Z_c = 1$  for  $Li^+$ ),  $C_0$  is the bulk salt concentration,  $F$  and  $J$  are Faraday's constant and the current density, respectively, and  $t_a$  is the transference number of anions.

**DFT calculations:** The calculations were performed within the framework of DFT, by using the projector augmented wave method as implemented in the Vienna ab Initio Simulation Package. The exchange-correlation energy was in the form of Perdew-Bruke-Ernzerhof. The cutoff energy for the plane-wave basis set was 500 eV, and  $2 \times 2 \times 1$   $\Gamma$ -centered k-point grids were used for the Brillouin zone integrations. For the surface systems, the bottom atom layers were fixed to simulate the body state, while the top atom layers were free to simulate the surface state. To reduce the interactions between each surface, a vacuum of 20 Å was contained in our calculation models. All structures were fully relaxed to the optimized geometry with the force convergence set at 0.01 eV/Å. To investigate the lowest energy configurations of adsorbed systems, we carefully manipulated structure parameters of the initial state (the distance, angle, and displacement between molecule and surface) to fully relax and selected the lowest energy result as the final state. The binding energy ( $E_{ads}$ ) of lithium adsorbing on the substrate materials is calculated referring to the following equation:

$$E_{ads} = E_{total} - E_{substrate materials} - E_{Li} \quad (S3)$$

where  $E_{total}$  is the total energy of substrate materials combined with lithium,  $E_{substrate materials}$  is the surface energy of POMs, solvents and TFSI,  $E_{Li}$  represents the energy of lithium in vacuum.

## 2. Supporting figures

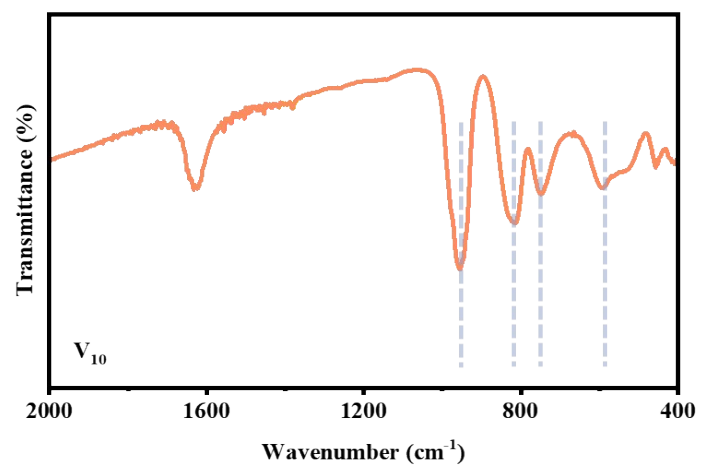


**Fig. S1.** FTIR spectra of V<sub>10</sub>.

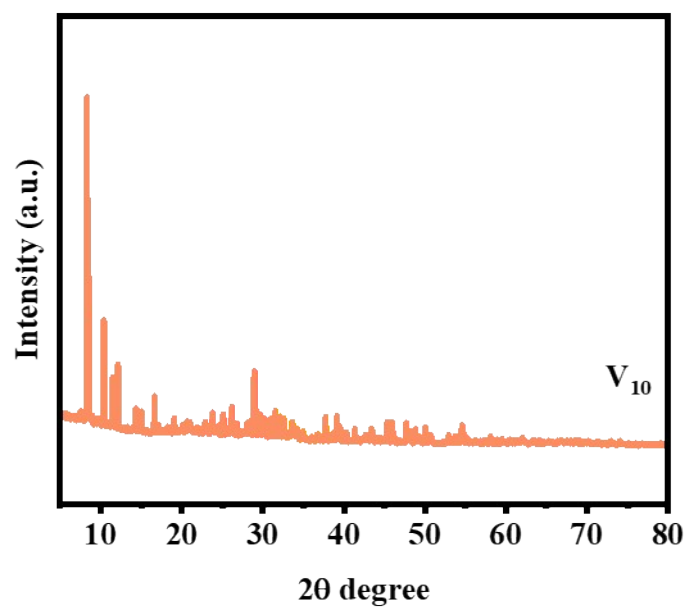


**Fig. S2.** XRD pattern of V<sub>10</sub>.

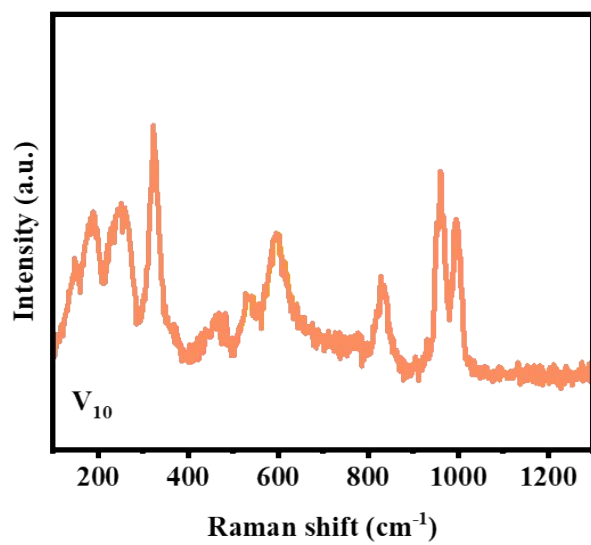


**Fig. S3.** Raman spectrum of V<sub>10</sub>.

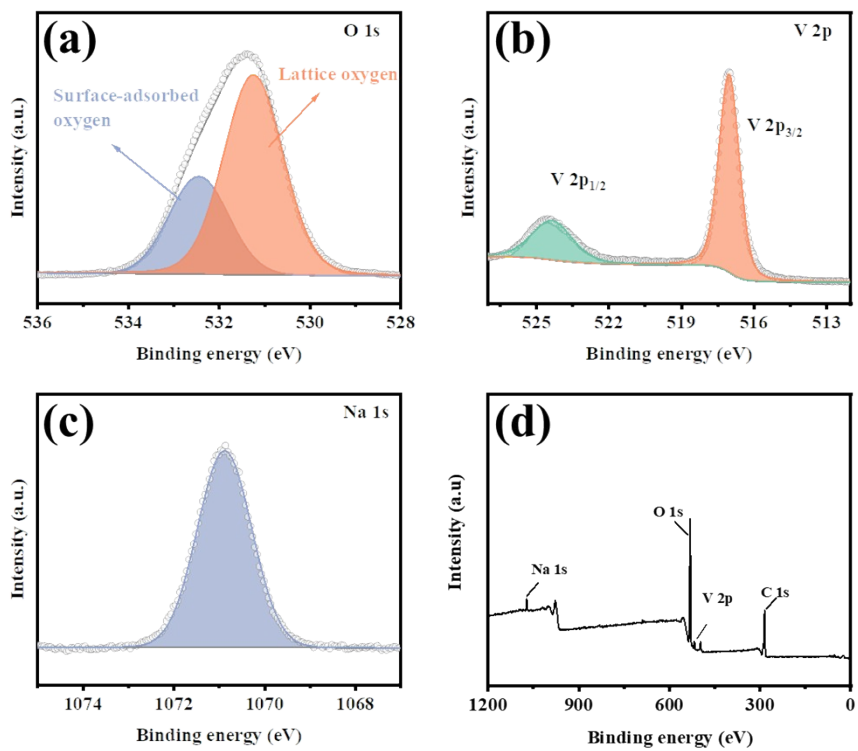


**Fig. S4.** XPS analyses of (a) O 1s, (b) V 2p, (c) Na 1s, and (d) full spectra for  $V_{10}$ .

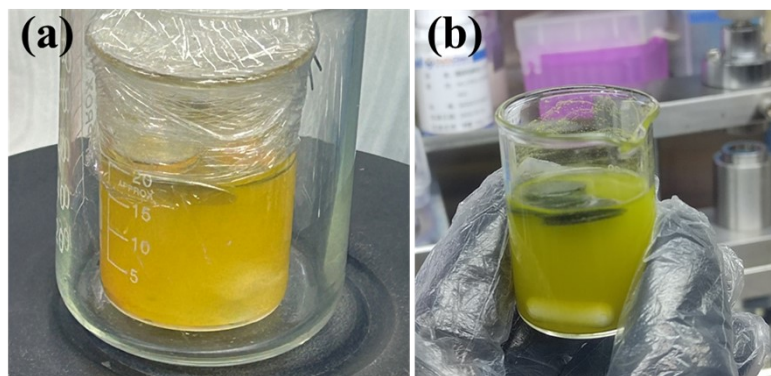


**Fig. S5.** Photos of (a) initial state and (b) after reaction time of 24 h.

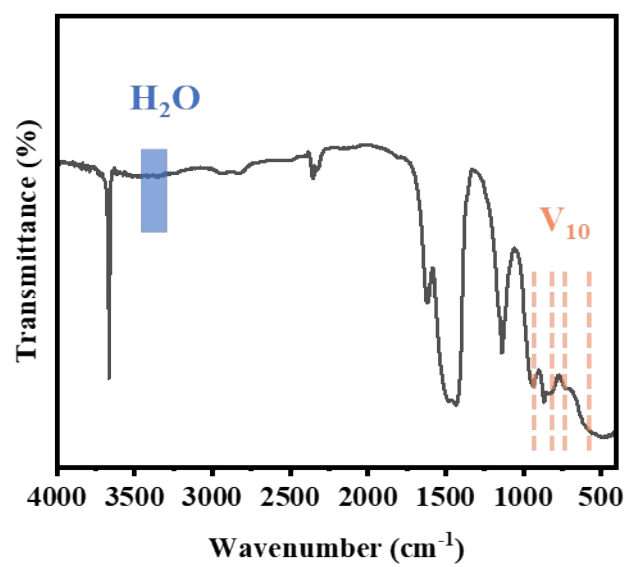


**Fig. S6.** FTIR spectra of V<sub>10</sub> ASEI layer. The absorption peak of H<sub>2</sub>O is approximately at 3400 cm<sup>-1</sup>.

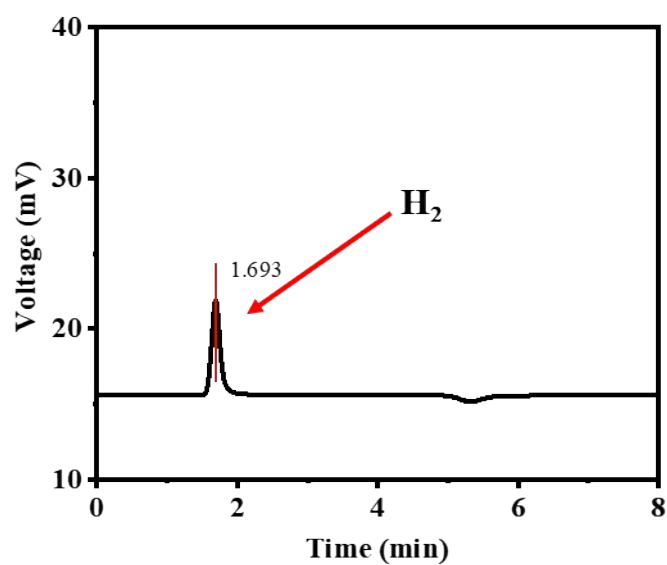


**Fig. S7.** Gas chromatography analysis of gases generated during the preparation of V<sub>10</sub> modified lithium foils.

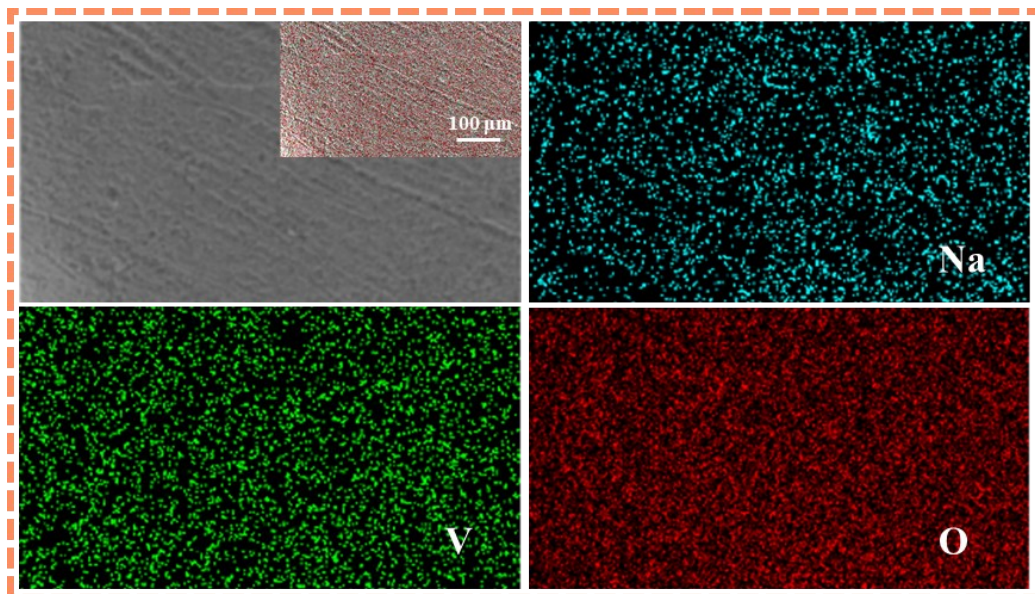


**Fig. S8.** The element mapping images of  $V_{10}$  modified lithium foil.

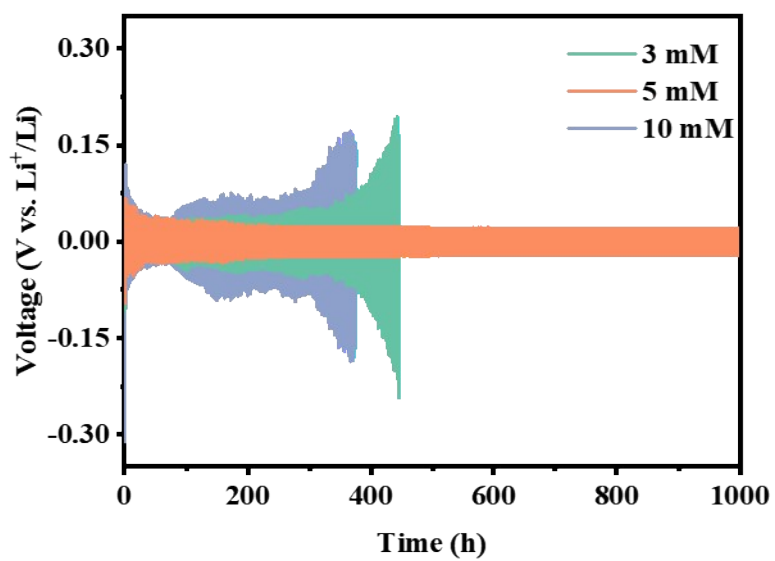


**Fig. S9.** Galvanostatic cycling at 1 mA cm<sup>-2</sup> with areal capacity of 1 mAh cm<sup>-2</sup>.

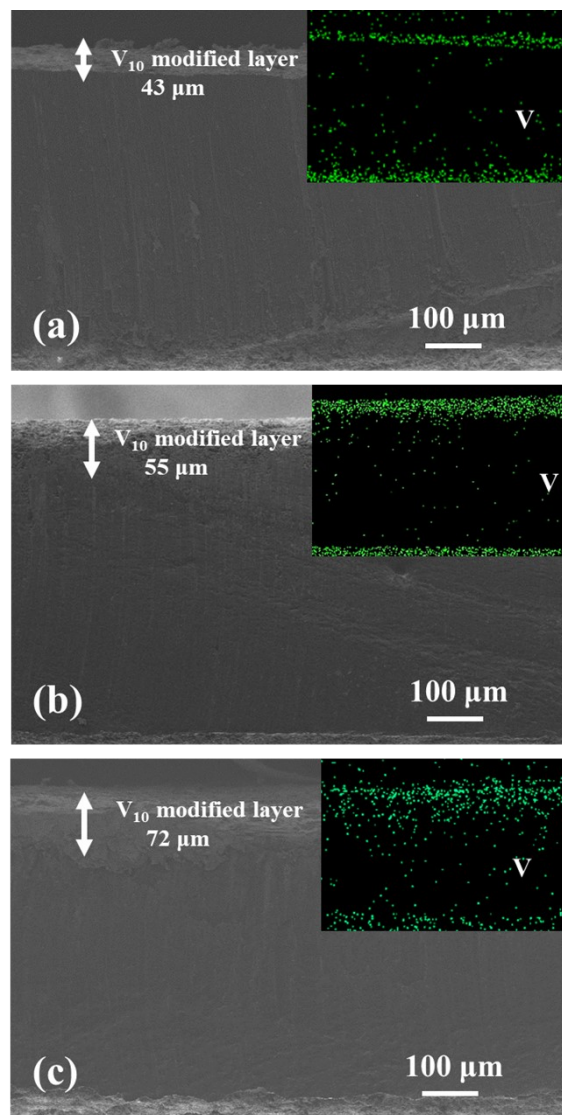


**Fig. S10.** The cross section SEM images of (a) 3 mM, (b) 5 mM, and (c) 10 mM  $V_{10}$  modified lithium foils (insets: element mapping images of cross section of  $V_{10}$  modified lithium foils).

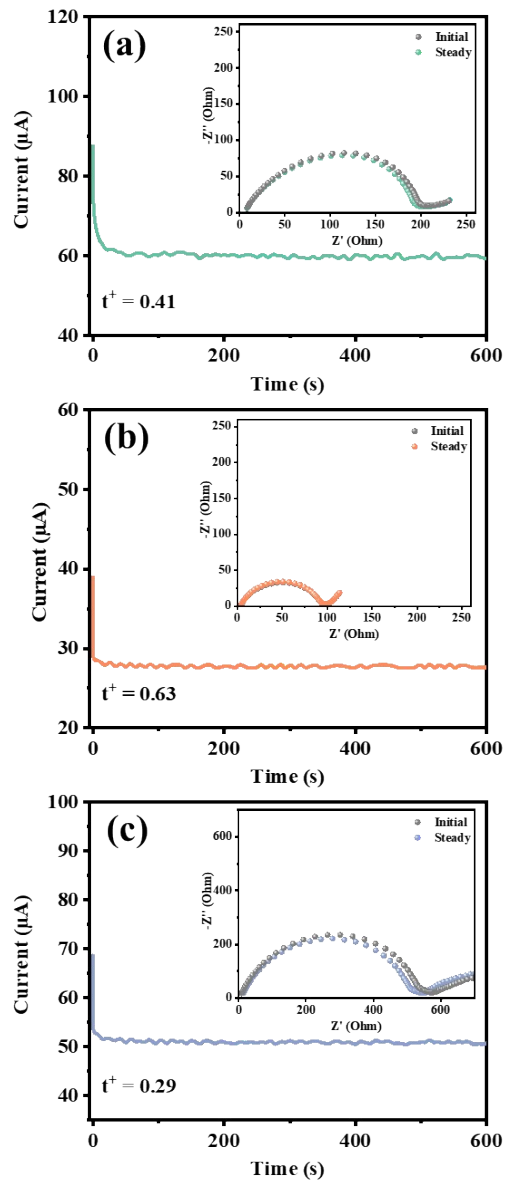


**Fig. S11.** Measurement of  $t_{\text{Li}^+}$  using potentiostatic polarization of Li//Li symmetric cells with (a) 3mM, (b) 5 mM, and (c) 10 mM  $V_{10}$  modified lithium foils (insets: Nyquist plots of impedance before and after polarization).

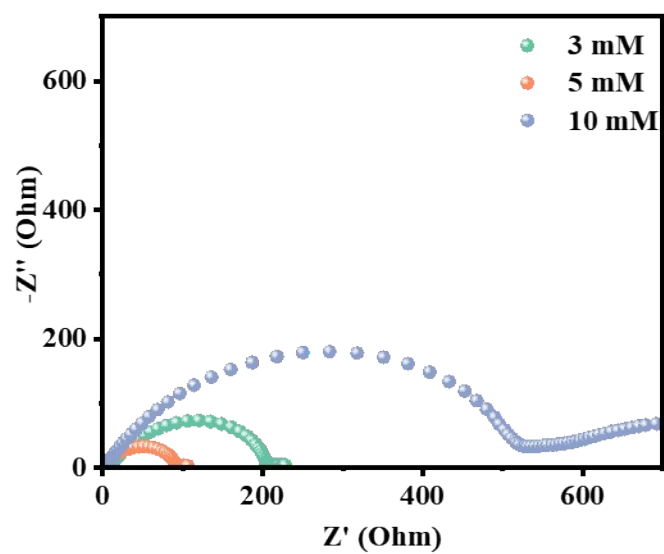


**Fig. S12.** EIS profiles of symmetrical cells using modified lithium foils with different concentrations of  $V_{10}$ .

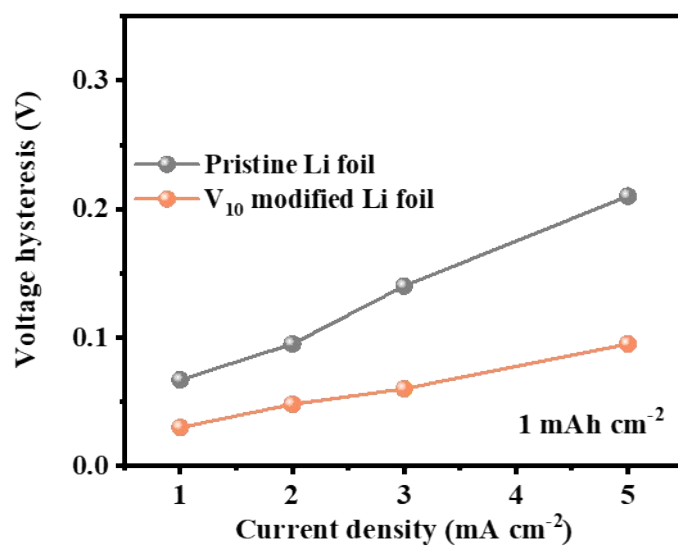


**Fig. S13.** (a) Voltage hysteresis of Li//Li symmetric cells with different Li foils at 1, 2, 3, and 5 mA cm<sup>-2</sup>.

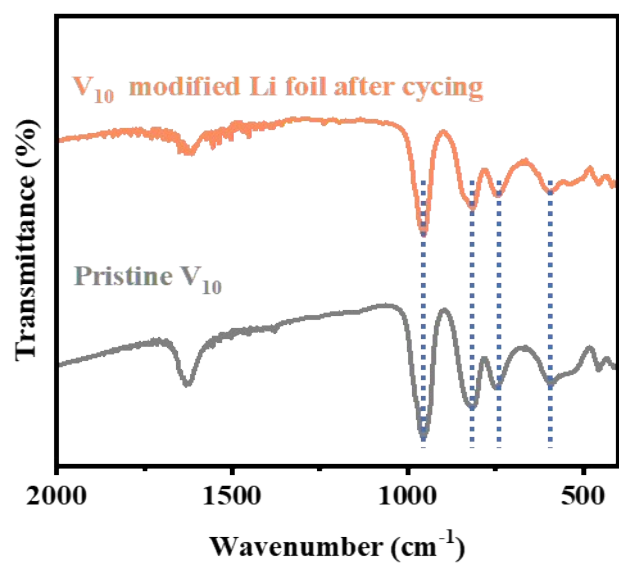


**Fig. S14.** FTIR spectra of V<sub>10</sub> modified lithium foil after cycling.

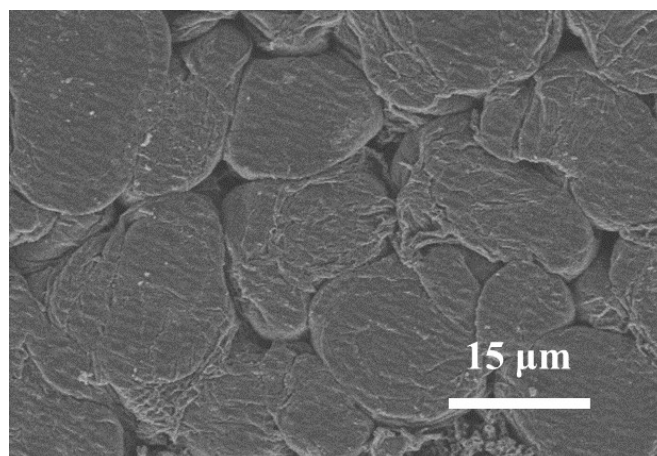


**Fig. S15.** SEM image of the surface of V<sub>10</sub> modified lithium foil after 50 h of cycling at 5 mA cm<sup>-2</sup> for 5 mAh cm<sup>-2</sup>.

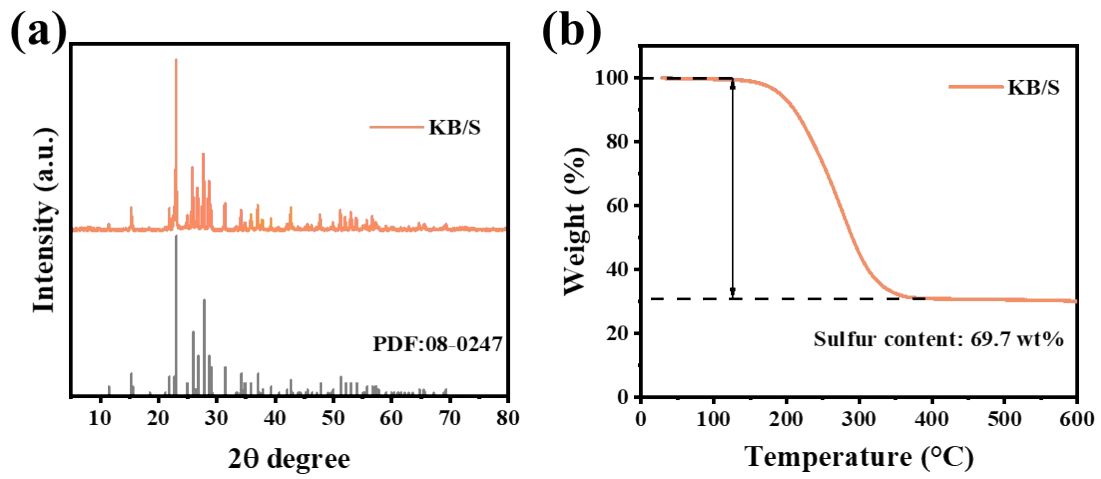


Fig. S16. (a) XRD pattern and (b) TGA curve of KB/S.